Electromagnetic Scattering from Grassland—Part I: A Fully Phase-Coherent Scattering Model

James M. Stiles, *Senior Member, IEEE,* and Kamal Sarabandi, *Senior Member, IEEE*

***Abstract*—A microwave scattering formulation is presented for grassland and other short vegetation canopies. The fact that the constituent elements of these targets can be as large as the vegetation layer make this formulation problematic. For example, a grass element may extend from the soil surface to the top of the canopy, and thus the upper portion of the element can be illuminated with far greater energy than the bottom. By modeling the long, thin elements of this type of vegetation as line dipole elements, this nonuniform illumination can be accounted for.**

Additionally, the stature and structure of grass plants can result in situations where the average inner-product or coherent terms are significant at lower frequencies. As a result, the backscattering coefficient cannot be modeled simply as the incoherent addition of the power from each element and scattering mechanism. To determine these coherent terms, a coherent model that considers scattered fields, and not power, is provided. This formulation is then used to provide a solution to the multiple coherent scattering terms, terms which include the correlation of the scattering between both dissimilar constituent elements and dissimilar scattering mechanisms.

Finally, a major component of the grass family are cultural grasses, such as wheat and barley. This vegetation is often planted in row structures, a periodic organization that can likewise result in significant coherent scattering effects, depending on the frequency and illumination pattern. Therefore, a formulation is also provided that accounts for the unique scattering of these structures.

***Index Terms*—Coherent scattering, extinction in random media, vegetation scattering models.**

I. Introduction

BECAUSE of their fundamental importance to Earth climate dynamics and the atmosphere's carbon cycle, forest vegetation has in recent years justifiably attracted the majority of interest in the field of microwave remote sensing of vegetation targets. However, another vegetation class that must not be overlooked is the category of grassland vegetation, both natural and cultural. As a significant portion of the Earth's dry surface is covered in grasses, a global understanding of the biophysical parameters which describe this vegetation is thus highly desirable, parameters that include soil moisture, biomass, and leaf area. Additionally, a significant amount of the cultivated land on the Earth's surface is occupied by members of the grass family. This fact leads to another motivation for determining globally accurate and timely descriptions of the Earth's cultural grasslands: The detection of drought, or the prediction of crop yields to estimate famine potential.

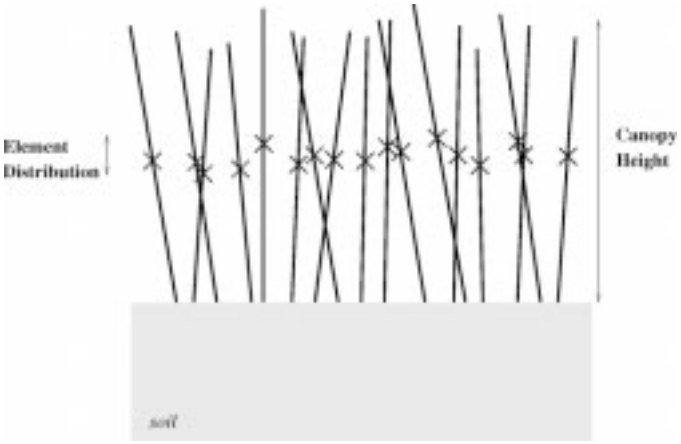

Fig. 1. Grass canopy consisting of long, thin elements. The vertical distribution of these elements (the center of each element is denoted by an "×") is much smaller than the overall canopy height.

Radar remote sensing can potentially be used to estimate these biophysical parameters, provided that the relationship between the physical parameters of grass vegetation and the resulting microwave scattering is well understood. However, both the structure and stature of grass vegetation lead to many unique problems that make the application of random media scattering techniques problematic. Grassland constituents are often neither axially straight nor circular in cross section, thus limiting the applicability of modeling grass plants as a collection of simple canonical elements where the scattering is well known. In addition, the relative position of the elements often cannot be described as uniformly distributed throughout the canopy layer. Instead, as demonstrated by the Fig. 1, the individual constituent elements can begin at the bottom of the scattering layer and traverse vertically to the top. The positions of these structures are often only slightly random in the vertical dimension, with a variance far smaller than the canopy height. As a result, it is difficult to model these structures as point targets within the scattering media, as the arbitrary reference used to derive structure location will greatly affect the scattering formulation.

This leads to the next problem associated with grassland scattering, that of the nonuniform illumination of the constituent elements. Since the long, thin elements of a grassland canopy extend from the top of the vegetation to the bottom, the coherent wave illuminating the element is nonuniform; that is, the intensity of the wave illuminating the element varies over the scattering element. Therefore, the scattering from a long element

Manuscript received November 14, 1997; revised November 10, 1998.

J. M. Stiles is with the Radar Systems and Remote Sensing Laboratory, The University of Kansas, Lawrence, KS 66045-2969 USA.

K. Sarabandi is with The Radiation Laboratory, The University of Michigan, Ann Arbor, MI 48109 USA.

Publisher Item Identifier S 0196-2892(00)00400-9.

within this layer is not simply an attenuated version of the scattering in freespace. The induced scattering currents will be modified, with the solution a function of the canopy within which it resides.

Finally, perhaps the most significant problem when dealing with grass canopies is the potential for the scattered *fields* from dissimilar elements to be significantly correlated. Both the stature and the structure of grassland elements lead to a case where field correlations can occur. The small stature of grass plants can result in an electrically small scattering volume in the microwave region. In other words, the volume wherein a single plant (and therefore its constituent elements) resides is electrically small in one or more dimensions. Additionally, the simple structure that defines most grass plants can lead to significant physical correlations between dissimilar elements. As a result, the total scattering power cannot be reduced to a summation of the scattering power from each separate plant element, but the plant structure as a whole must be considered [1]–[6]. Likewise, the row structures in which cultural grasses such as wheat or barley are planted also lead to coherent effects that must be accurately represented in the scattering model.

Therefore, this paper presents a microwave scattering model for grassland vegetation, wherein the problems of arbitrary constituent shape, nonuniform illumination, and phase-coherent effects are accounted for. The model is therefore a departure from many other grassland scattering models, which largely use phase-incoherent solutions such as radiative transfer [7]–[9], model grass constituents as simple structures [3], [7]–[10], and/or uniformly distribute the constituent locations throughout the vegetation layer [7]–[10].

II. Single-Element Scattering

The first step in formulating the scattering from grassland canopies is to determine the scattering response from the long, thin dielectric elements (stalks, blades) that are the constituent elements of grassland vegetation. Specifically, we seek a formulation for the scattered field from a long, thin element of arbitrary shape and cross section that is located in a extinction layer (vegetation) over a rough dielectric half space (soil). It has been shown that the scattering from long, thin dielectric elements can be attributed to electric line-dipoles lying along the cylinder axis [11], [12], provided that the element diameter is small compared to the field wavelength. The total scattering from the cylinder can be thought of as a coherent addition (integration) of the scattering from incremental or differential dipoles along the thin element, with a dipole moment described as $\boldsymbol{p}_{2d}\,d\ell$, where $d\ell$ is the differential distance along the long cylinder axis. It should be noted that the dipole moment of a short element (length $\Delta\ell \ll \lambda$) cannot be determined from $\boldsymbol{p}_{2d}$ (i.e., $\boldsymbol{p} \neq \boldsymbol{p}_{2d}\Delta\ell$). The dipole moment $\boldsymbol{p}_{2d}$ is a function of the incident electric field along the element axis, as well as of the two-dimensional polarizability tensor $\mathcal{P}_{2d}$. A scattering matrix element for an incremental dipole (in free space) is thus determined from the scattering matrix element of a standard dipole [13, pp. 91-92]

$$S_{\chi\psi}\,d\ell = \frac{k_0^2}{4\pi}\hat{\chi}_s(\hat{k}^i)\cdot\mathcal{P}_{2d}\,d\ell\cdot\hat{\psi}_i(\hat{k}^i) \tag{1}$$

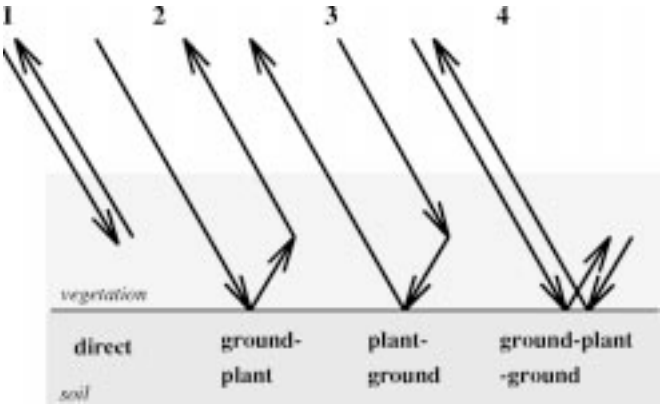

Fig. 2. The four first-order scattering mechanisms to be considered in this scattering formulation.

where S is an element of the scattering matrix for orthogonal receive/transmit polarization vectors $\hat{\chi}$, $\hat{\psi}$, vectors that are dependent on the incident direction vector $\hat{k}^i = \cos\phi_i \sin\theta_i + \sin\phi_i \sin\theta_i + \cos\theta_i$.

The scattered field associated with this dipole element is of course proportional to the local incident field, and thus a representation of the incident field at every location along the thin grassland element must be determined. Since these elements reside in an extinction layer (the vegetation canopy), this incident field is not a uniform plane wave, but one whose intensity varies across the grass element, diminishing as the vertical depth within the layer increases. The incident field is thus dependent on the extinction exhibited by the vegetation layer, as well as the position within that layer. Likewise, the far-field scattering response from an elemental dipole along the long, thin grass element is modified by the propagation path from the dipole element back through the vegetation layer. Thus, we must first determine a formulation for coherent propagation to/from an arbitrary point within the vegetation layer.

This formulation will consider only first-order scattering mechanisms, of which there are four: a direct scattering term, two ground bounce terms, and a double-bounce term (Fig. 2). The total scattered *field* is therefore the *coherent* summation of these four terms. To determine this value correctly, each of the four scattering mechanisms must be referenced to a single equi-phase plane. The propagation by each of the four scattering mechanisms can be modeled as a sum of two complex propagation paths, the direct path Φ_1 and the reflected or image path Φ_2 (Fig. 3). Fig. 4 shows the geometry of the direct path, where the equi-phase plane is arbitrarily taken to pass through the origin. Using ray optics, the propagation path from the equi-phase plane directly to position $\overline{r}'$ is therefore

$$\begin{aligned}\Phi_1(\overline{r}') &= (\overline{r}_1 - \overline{r}_p)\cdot\overline{k}_0 + (\overline{r}' - \overline{r}_1)\cdot\overline{k}_1 \\ &= \overline{r}_1\cdot\overline{k}_0 + (\overline{r}' - \overline{r}_1)\cdot\overline{k}_1\end{aligned} \tag{2}$$

where $\overline{r}_1$ defines the location where the ray intersects the top of the vegetation layer and $\overline{r}_p$ defines the location where the ray intersects the equi-phase plane. The vector $\overline{k}_0$ specifies the incident plane wave in free space, propagating in the direction θ_i, ϕ_i and is defined as

$$\overline{k}_0 = k_0^x\hat{x} + k_0^y\hat{y} + k_0^z\hat{z} \tag{3}$$

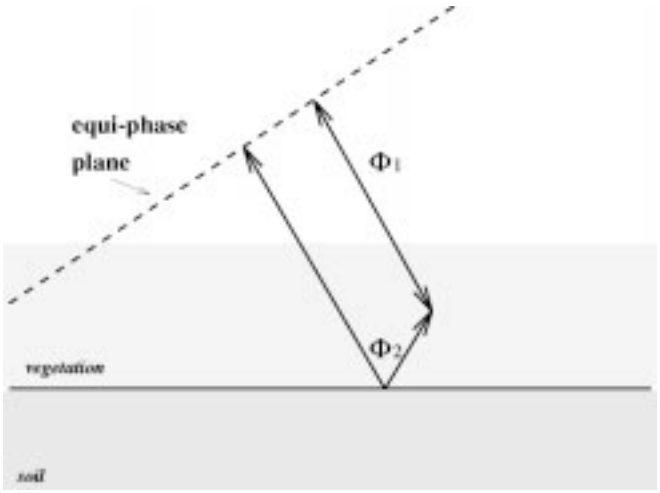

Fig. 3. Propagation paths of each of the four first-order scattering mechanisms can be constructed in terms of the propagation along paths Φ_1 and/or Φ_2. Since a coherent field solution is desired, these paths must be referenced to a single, equi-phase plane.

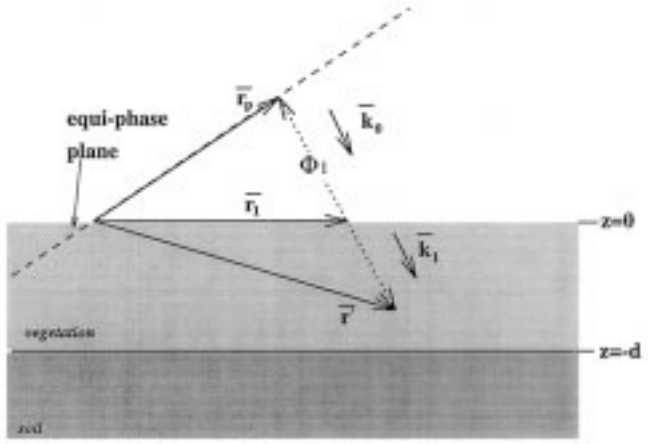

Fig. 4. Propagation along path Φ_1 is the propagation from the equi-phase plane to the canopy surface in free space $((\overline{r}_1 - \overline{r}_p) \cdot \overline{k}_0)$ and the propagation from the canopy top to the scatterer in the grass vegetation $((\overline{r}' - \overline{r}_1) \cdot \overline{k}_1)$.

where

$k_0^x = k_0 \cos\phi_i \sin\theta_i$;
$k_0^y = k_0 \sin\phi_i \sin\theta_i$;
$k_0^z = k_0 \cos\theta_i$.

Additionally, $\overline{k}_1 = k_1 \hat{k}_0$ where k_1 is the effective propagation constant of the sparse vegetation canopy, a complex value that specifies both the attenuation and phase velocity of the coherent (average) wave within the medium. Note this formulation implies a diffuse boundary condition at the air/vegetation interface, such that the direction of propagation in the grass layer is evaluated as that of free space.

The propagation of an electromagnetic field within the vegetation layer can therefore be described as $\exp[\imath\Phi_1(\overline{r}')]$ where $\Phi_1(\overline{r}')$ is, after further evaluation, determined to be

$$\Phi_1(\overline{r}') = k_0^x x' + k_0^y y' - \frac{k_\rho^2 z'}{k_0 \cos\theta_i} + \frac{k_1 z'}{\cos\theta_i} \tag{4}$$

where $\overline{r}'$ is a point within the scattering layer and $k_\rho^2 = (k_0^x)^2 + (k_0^y)^2$.

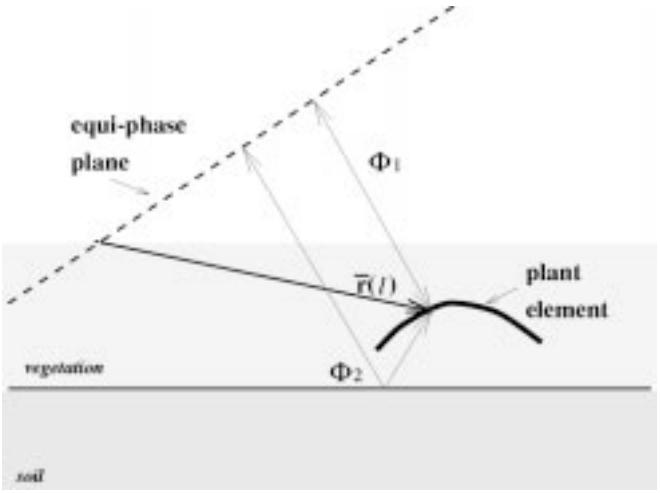

Fig. 5. Transmission and scattering propagation paths can be determined at every position $\overline{r}(\ell)$ along a thin grass element. The differential dipole moment at every location along the thin element can therefore be computed.

Using the same procedure as for Φ_1, the image, or ground bounce term Φ_2 is found to be

$$\Phi_2(\overline{r}') = k_0^x x' + k_0^y y' + \frac{k_\rho^2 (z' + 2d)}{k_0 \cos\theta} - \frac{k_1 (z' + 2d)}{\cos\theta} \tag{5}$$

with the propagation in the vegetation described as $R \exp[\imath\Phi_2(\overline{r}')]$. The value R is the appropriate coherent reflection coefficient for the rough soil, an artifact of the spicular ground reflection encountered by this image path.

These two propagation expressions can be used in combination to determine the relative propagation of the coherent electric field from the equi-phase plane, to an arbitrary location within the canopy, and back to the equi-phase plane for any of the four first-order scattering mechanisms shown in Fig. 2. The arbitrary location, for example, could be a location on a thin dielectric (i.e., grassland) structure, specifying therefore the position of an incremental dipole element, as shown in Fig. 5. The scattering from an entire thin dielectric element is thus determined by integrating the scattering from a differential dipole element (1) over the contour C of the element axis

$$S_{\chi\psi}^{mech} = \frac{k_0^2}{4\pi} \int_C \hat{\chi}_{mech}(\hat{k}^i) \cdot \mathcal{P}_{2d}(\overline{r}(\ell)) \cdot \hat{\psi}_{mech}(\hat{k}^i)\, \Phi_{\chi\psi}^{mech}(\hat{k}^i; \overline{r}(\ell))\, d\ell \tag{6}$$

where

$mech$ — one of the four first-order scattering mechanisms ($mech \in \{1, 2, 3, 4\}$);

$\overline{r}(\ell)$ — a position vector that denotes the location on the element using the parametric variable ℓ;

$\Phi_{\chi\psi}^{mech}(\hat{k}^i; \overline{r}(\ell))$ — specifies the propagation from the equi-phase plane to location $\overline{r}(\ell)$ and back again, using the proper combinations of (4) and (5).

For the specific expressions of $\Phi_{\chi\psi}^{mech}$ pertaining to each of the four scattering mechanisms, refer to the Appendix of this paper.

Again, the scattering from the long, thin dielectric elements found in grassland canopies can be evaluated in this manner

because the scattering from these structures is attributed to line dipoles along the contour of the element. These incremental dipoles couple very weakly with each other, so that (6) is an asymptotically valid expression regardless of the electrical length of the long dielectric element [12]. As a result, the above expression is also used to approximate the scattering from cylinders with moderate axial curvature (the coupling effects are still slight), a form exhibited by many constituents of grassland canopies.

The total first-order scattering from this grassland element is therefore the coherent sum of the four first-order scattering terms

$$S_{\chi\psi} = \sum_{mech=1}^{4} S_{\chi\psi}^{mech}. \tag{7}$$

Several points should be emphasized about this formulation. The first is that this solution provides the coherent addition of the scattered *fields* for each of the four first-order scattering mechanisms, rather than the scattered *power*, the parameter most often evaluated. Additionally, the solution allows for thin elements of moderate curvature and can accurately evaluate arbitrarily shaped cross sections if the corresponding polarizability tensor $\mathcal{P}_{2d}$ is known.

Another important point about this solution is its completeness. This is not a solution for the scattering of a thin dielectric element, but instead of a dielectric element in an extinction layer over a dielectric half space. The effect of the extinction layer and the reflection from the half space are comprehended in the solution. As a result, the formulation is not only dependent on the usual elemental parameters such as size, shape, orientation, and dielectric properties, but on its *position* within the layer as well. This is true for its vertical position denoted by z, but also for the relative phase associated with its lateral position, denote*d by x and y.

Finally, perhaps the most significant aspect of this model is that it accurately represents the illumination of the element by the coherent wave. Since the propagation both to and from each arbitrary point on the scatterer is determined, the effect of the extinction layer on the scattering element is accurately represented. This is particularly true for thin elements that extend from the top of the extinction layer, where it is intensely illuminated, to the bottom of the layer, where it may be barely illuminated by the incident wave. This effect can be profound, as the result is a scattering *pattern*, which is significantly different than that produced by a uniform illumination. That is, the scattering formulation is not simply an attenuated (by the vegetation) version of the free-space scattering, but instead results in a solution where the direction, as well as intensity, of the scattered energy is modified by the canopy extinction.

III. Average Scattered Power

The previous section provides a solution for computing the scattered electric field (in the far field) for a constituent element in an extinction layer over a dielectric half space. However, for applications involving the remote sensing of random media, the parameter of interest is not the scattered field of a fixed element, but instead can be specified in general as the average *covariance* of the scattered fields from an element or elements whose parameters are defined by a set of random variables, including position, orientation, size, and shape. This parameter is denoted as $\langle S_{\chi\psi} S_{\lambda\mu}^{*} \rangle$ where $\chi\psi$ and $\lambda\mu$ denote arbitrary receive/transmit polarizations (e.g.,$\{vv, hv, vh, hh\}$), $*$ denotes complex conjugate, and $\langle\,\rangle$ denotes the expected value operation over all random variables describing the element. A complete average covariance matrix can be constructed [14, p. 31] by calculating a set of these values for all possible polarization combinations, which completely characterizes the average scattering from a random media. The diagonal terms of the covariance matrix are real valued and represent the average scattered power for each of the four polarization states. From (7), this is given as

$$\langle |S_{\chi\psi}|^2 \rangle = \sum_{mech=1}^{4} \sum_{mech'=1}^{4} \langle S_{\chi\psi}^{mech} S_{\chi\psi}^{*mech'} \rangle. \tag{8}$$

There are thus 16 terms required to determine the total power, four of which ($mech = mech'$) represent the incoherent power, the scattered power from each scattering mechanism being considered independently. The remaining 12 inner product terms can either add to, or detract from, the incoherent power value and represent the correlation between the scattered fields of dissimilar scattering mechanisms. For many cases, the correlation is small and the 12 inner product terms are insignificant when compared to the incoherent power. However, this is true only under specific conditions, and thus for this formulation these terms will be maintained.

The structure of the grass plant to be modeled will consist of, completely or partially, three basic elements; namely leaf, stalk, and grain elements (Fig. 6). The leaf and stalk will be modeled as line-dipole elements, whereas the grain model is evaluated as a point target. Using first-order discrete scattering theory (i.e., no constituent coupling), the scattered field from a grass plant

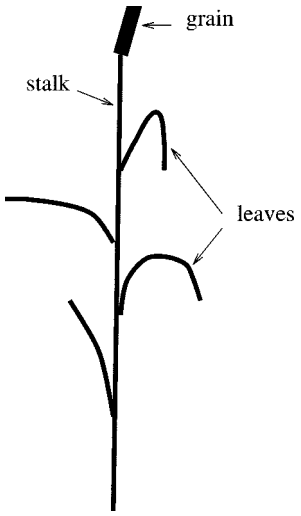

Fig. 6. The three grass plant constituent elements considered in this model: A stalk, the grain element, and multiple leaf elements. The leaf and stalk elements are long, thin dielectric structures that can exhibit axial curvature and arbitrary cross sections.

can be expressed as the coherent sum of the scattering from its constituent elements

$$S_{\chi\psi}^{plant} = S_{\chi\psi}^{grain} + S_{\chi\psi}^{stalk} + \sum_{n=1}^{N} S_{\chi\psi}^{leaf\ n}. \tag{9}$$

A general element of the covariance matrix for the scattering from an entire plant can thus be written as

$$\begin{aligned}\langle S_{\chi\psi}^{plant} S_{\lambda\mu}^{*plant}\rangle &= \langle S_{\chi\psi}^{grain} S_{\lambda\mu}^{*grain}\rangle + \langle S_{\chi\psi}^{stalk} S_{\lambda\mu}^{*stalk}\rangle \\ &\quad + \sum_{n=1}^{N} \langle S_{\chi\psi}^{leaf\ n} S_{\lambda\mu}^{*leaf\ n}\rangle + \langle S_{\chi\psi}^{grain} S_{\lambda\mu}^{*stalk}\rangle \\ &\quad + \langle S_{\chi\psi}^{stalk} S_{\lambda\mu}^{*grain}\rangle + \sum_{n=1}^{N} \langle S_{\chi\psi}^{grain} S_{\lambda\mu}^{*leaf\ n}\rangle \\ &\quad + \sum_{n=1}^{N} \langle S_{\chi\psi}^{stalk} S_{\lambda\mu}^{*leaf\ n}\rangle \\ &\quad + \sum_{n=1}^{N} \langle S_{\chi\psi}^{leaf\ n} S_{\lambda\mu}^{*grain}\rangle \\ &\quad + \sum_{n=1}^{N} \langle S_{\chi\psi}^{leaf\ n} S_{\lambda\mu}^{*stalk}\rangle \\ &\quad + \sum_{n=1}^{N} \sum_{m\neq n}^{N} \langle S_{\chi\psi}^{leaf\ n} S_{\lambda\mu}^{*leaf\ m}\rangle \end{aligned} \tag{10}$$

where $\chi\psi$ and $\lambda\mu$ again represent an arbitrary element of set $\{vv, vh, hv, hh\}$. Equation (10) represents a startling number of terms, as the correlation between dissimilar constituent elements is considered. If $\chi\psi = \lambda\mu$, then the covariance elements represent real scattered power $\langle|S^{plant}|^2\rangle$, with the first three terms of (10) providing the incoherent scattering power and the remaining terms providing the inner product or coherent scattering power. If the plant contains four leaves, then the number of incoherent terms totals 24 (six elements, and four mechanisms). This is contrasted to the coherent formulation of (10), where $24^2 = 576$ terms, including the 24 incoherent terms, are represented. These incoherent values are generally the most significant individual terms of (10), and this fact is often used to justify neglecting the coherent terms of (10). However, the question is not whether the incoherent terms are the greatest single terms, but whether the remaining 552 coherent terms are insignificant when taken in total.

For electrically large and very random vegetation, the coherent terms, even when taken in total, will likely be small and thus the coherent power can be discarded. However, the small stature and simple structure of a grass plant can result in scattering scenarios where these coherent effects cannot be disregarded. The effective scattering volume of a single plant may be sufficiently small such that the relative phase variation across the volume is less than 2π (particularly for low frequencies). Therefore, random scatterers within the volume may still produce scattered fields that are generally aligned in phase and thus significantly correlated. Additionally, the constituent scatterers of a simple grass plant are often physically well correlated (e.g., leaves located along the stalk, grain at the stalk apex, etc.), which further increases the correlation of their resulting scattered fields. Essentially, these relatively small and simple plants at times must be evaluated as individual scattering elements; they cannot be segmented into smaller constituent elements for evaluation by incoherent scattering formulations.

IV. Constituent Models

In several previous cases [7]–[10], the leaf elements of grassland constituents have been modeled as straight elements and/or as elements with circular or elliptical cross sections. However, the effect of the approximation on model accuracy is uncertain as the leaf or blade structures of grass plants are curved elements with decidedly noncircular cross sections. As one goal of this study has been to produce accurate constituent scattering models in both the electromagnetic and plant fidelity senses, we seek to find a solution that better represents this observed structure. Both the leaf and stalk constituents are essentially long, thin dielectric elements. It will be assumed that the radius of these structures is small with respect to a wavelength, their curvature moderate, and their axial ratio (length to radius) is large such that the scattering formulations presented in this paper can be implemented. These assumptions are not considered to be a major restriction when evaluating most grassland vegetation in the microwave frequency region.

To implement the scattering solution of a thin dielectric element such as a stalk, essentially two items must be defined. The first is the polarizability tensor element $\mathcal{P}_{2d}$ that accounts for the dielectric and cross section of the element, while the other is the vector $\overline{r}_{stalk}$, which defines the axial contour of the thin scattering element. A stalk element is modeled as a straight element originating at location $-d\hat{z}$, so the contour vector is given as

$$\begin{aligned}\overline{r}_{stalk} &= \cos\phi_{stalk} a(z+d)\hat{x} \\ &\quad + \sin\phi_{stalk} a(z+d)\hat{y} + z\hat{z} \quad -d < z < z_0. \end{aligned} \tag{11}$$

As shown by Fig. 7, the element is tilted at an angle $\theta = \tan^{-1} a$ in the azimuthal direction ϕ_{stalk}, and thus the length of the element is $\sqrt{1+a^2}(z_0+d)$, where z_0 is the vertical position of the top of the stalk. Additionally, the diameter of the stalk is not necessarily constant, but instead can taper with height. The cross-sectional area is thus a function of z, which again can be accounted for completely with a polarizability tensor function $\mathcal{P}_{2d}(z)$.

For leaf elements of many grasses such as wheat, the cross section can be described, generally, as blade shaped, a cross section for which polarizability tensors $\mathcal{P}_{2d}$ have been computed [15]. The contour vector representation for a leaf element is more complex than for the stalk. Two vectors must be defined, one that locates the leaf element on the stalk ($\overline{r}_{ref}$), and another that specifies the leaf contour ($\overline{r}'$). Because the implemented scattering model is coherent, with the correlation between dissimilar elements computed, the relative position of plant elements must be accurately represented. For example, a leaf element will always emanate from the stalk, and therefore the leaf contour must reflect this fact. As shown in Fig. 8, vector $\overline{r}_{ref}$ specifies the point where a leaf element attaches to the stalk. If

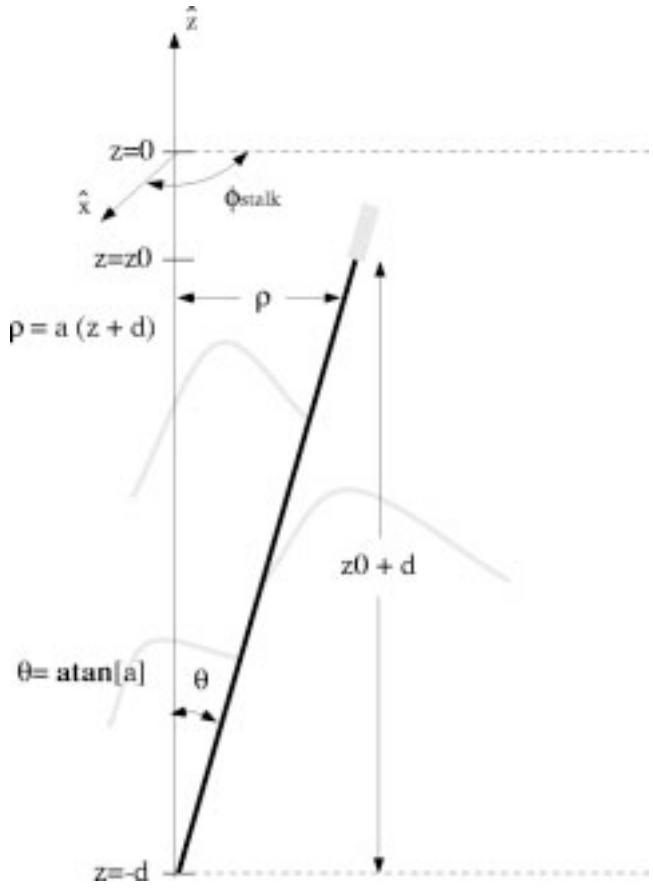

Fig. 7. Geometry of the stalk model demonstrating the variables z_0, a, and ϕ_{stalk}.

the vertical position of the leaf element is specified by (random) variable z_{ref}, then from (11)

$$\overline{r}_{ref} = \cos\,\phi_{stalk} a(d + z_{ref})\hat{x} + \sin\,\phi_{stalk} a(d + z_{ref})\hat{y} + z_{ref}\hat{z}. \quad (12)$$

To provide a more accurate representation of the curvature of the leaf, the second-order polynomial $z = c_1\rho - (c_2\rho)^2$ $(0 < \rho < \rho_0)$ was chosen as an approximation of naturally occurring elements (Fig. 9). Note the base of the element originates from the origin ($\rho = 0$, $z = 0$), therefore defining a new (primed) coordinate system at location $\overline{r}_{ref}$. If the leaf azimuthal orientation is defined as ϕ_{leaf}, the contour vector for a leaf element can be described as the sum of $\overline{r}_{ref}$ and $\overline{r}'$

$$\overline{r}_{leaf} = \overline{r}_{ref} + \rho' \cos\,\phi'_{leaf}\hat{x} + \rho' \sin\,\phi'_{leaf}\hat{y} + \left(c_1\rho' - (c_2\rho')^2\right)\hat{z} \qquad 0 \le \rho' \le \rho_0. \quad (13)$$

The grain element is modeled as a circular dielectric cylinder of length h_{grain} and radius a_{grain}. Again, the position of this element relative to the plant must be determined. Since the grain element is located at the apex of the stalk element (Fig. 10), the vertical position of the center of a grain element is $z = z_0 + 0.5h_{grain}\cos\,\beta$. The angle β is generally small, such that $\cos\,\beta \approx 1$, and thus the position vector describing the grain location is found from (11)

$$\overline{r}_{grain} = \cos\,\phi_{stalk} a(z_0 + h_{grain}/2 + d)\hat{x} + \sin\,\phi_{stalk} a(z_0 + h_{grain}/2 + d)\hat{y} + (z_0 + h_{grain}/2)\hat{z}. \quad (14)$$

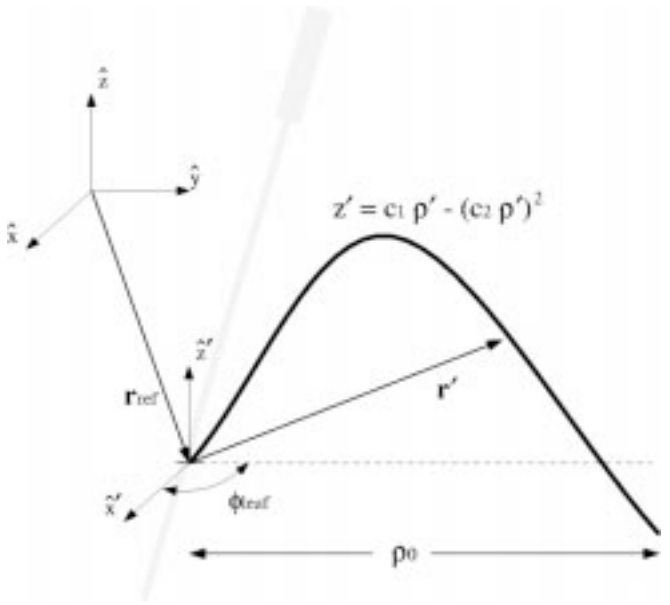

Fig. 8. Geometry of leaf model, demonstrating vector $\overline{r}'$ and variables z_{ref}, ϕ_{leaf}, c_1, c_2, and ρ_0.

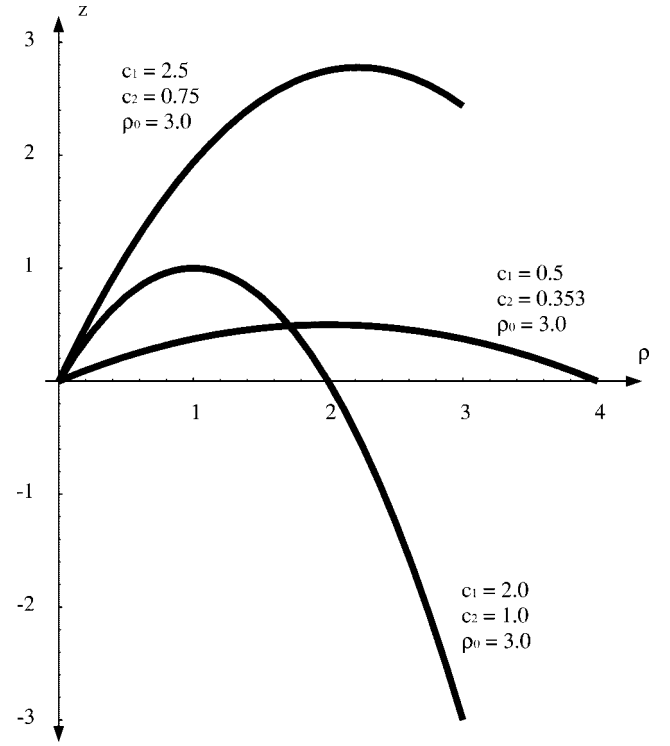

Fig. 9. Demonstration of leaf curvature model for three sets of curvature parameters $\{c_1, c_2, \rho_0\}$.

The parameters that appear in the above constituent model equations are of course random variables when considering an entire wheat or other grassland canopy. Therefore, the statistical moments and covariances describing this set of random variables must be defined before the scattering covariance elements can be computed. Because coherent scattering terms are

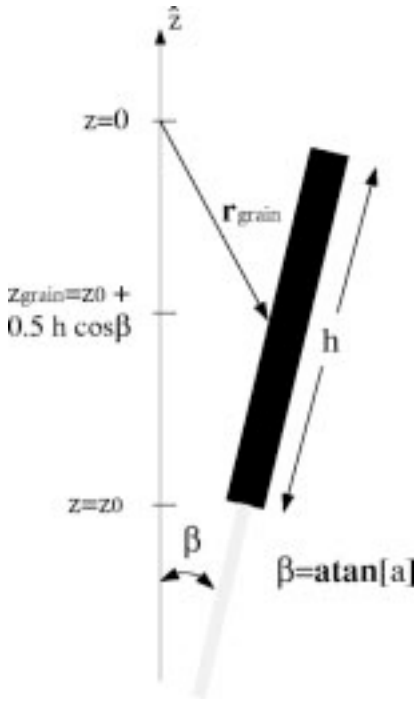

Fig. 10. Geometry of grain model demonstrating grain variables h and β.

to be evaluated, joint probability density functions involving parameters from dissimilar constituent elements must be described, along with the corresponding parameter covariances. For example, since leaf and grain elements must be attached to the center stalk element, the positions of leaves and grain are dependent on the random variables describing the stalk. This dependence must be explicitly stated in order to calculate coherent scattering terms. Additionally, the statistical descriptions of plant locations within a row-structured canopy must be specified, so that the coherent effects of row structure can be evaluated.

V. Scattering from Cultural Grass Canopies

The preceding sections have provided a solution for the average scattering from a single plant residing in the vegetation layer. However, the desired solution is the average scattering from an entire grassland canopy, a random collection of individual plants. Similar to plant scattering, the scattering from a canopy can be modeled as the coherent sum of the scattering from individual plants. Consider planar area A containing N grass plants, the location of each denoted by vector $\overline{\rho}^n_{plant}$. The scattered electric field can be represented in the far field as

$$S^{canopy}_{\chi\psi} = \sum_{n=1}^{N} S^{plant}_{\chi\psi\, n}\Theta(\overline{\rho}^n_{plant}) \tag{15}$$

where $S^{plant}_{\chi\psi\, n}$ is likewise the coherent sum of all four scattering mechanisms and $\Theta(\overline{\rho}^n_{plant}) = \exp[i2k_0\hat{k}^i_\rho \cdot \overline{\rho}^n_{plant}]$ is the relative phase of the plant.

If the plant scattering is assumed independent of both its location and the other plants, the covariance matrix elements representing the scattering from this area is

$$\begin{aligned}\langle S^{canopy}_{\chi\psi} S^{*canopy}_{\lambda\mu}\rangle = &\sum_{n=1}^{N}\langle S^{plant}_{\chi\psi} S^{*plant}_{\lambda\mu}\rangle_n \\ &+ \sum_{n=1}^{N}\sum_{m\neq n}^{M}\langle S^{plant}_{\chi\psi\, n}\rangle\langle S^{*plant}_{\lambda\mu\, m}\rangle \\ &\cdot\langle\Theta(\overline{\rho}^n_{plant})\Theta^*(\overline{\rho}^m_{plant})\rangle \\ &+ \langle S^{soil}_{\chi\psi} S^{*soil}_{\lambda\mu}\rangle\end{aligned} \tag{16}$$

where $\langle S^{plant}_{\chi\psi\, n}\rangle$ is the average scattered field from a single plant. For similar polarization pairs ($\chi\psi = \lambda\mu$), (16) again is interpreted as the incoherent scattered power; that is, the summation of the scattered power from each plant, plus the coherent power terms due to the correlation of scattered fields from dissimilar plants. Although generally ignored, the coherent term can be a significant portion of the total scattered power, depending on the specific scattering scenario. Note the additional term $\langle S^{soil}_{\chi\psi} S^{*soil}_{\lambda\mu}\rangle$ appears at the end of the above equation. This term accounts for the direct backscattered energy from the rough soil surface, with the propagation through the vegetation layer properly considered.

Many of the plants comprising the grass family, such as wheat and barley, are agricultural crops that grow not in a random fashion but instead are planted in relatively straight, periodic rows. The coherent scattering term can be greatly influenced by this structure [16], [17], and the coherent solution for this distribution will be presented here. To begin, we first consider the scattering from a section of a single row, located at $x = 0$ and extending from $y_{\min} < y < y_{\max}$. The plant locations are assumed to be uniformly distributed in y, with a Gaussian distribution in x (defined by variance σ_x^2). The scattering covariance from this row section can be expressed as

$$\begin{aligned}\langle S^{row}_{\chi\psi} S^{*row}_{\lambda\mu}\rangle = &N_p\langle S^{plant}_{\chi\psi} S^{*plant}_{\lambda\mu}\rangle \\ &+ N_p(N_p-1)\langle S^{plant}_{\chi\psi}\rangle\langle S^{*plant}_{\lambda\mu}\rangle \\ &\cdot\langle\exp[i2k_0\overline{k}_\rho\cdot(\overline{\rho}_n-\overline{\rho}_m)]\rangle_{n\neq m}\end{aligned} \tag{17}$$

where the two terms can again be interpreted as incoherent and coherent scattering. Since the scattering from a single plant is independent of its location, the row structure will numerically affect only the phase function $\langle\exp[i2k_0\overline{k}_\rho\cdot(\overline{\rho}_n-\overline{\rho}_m)]\rangle_{n\neq m}$. Again assuming that the $\hat{x}$ and $\hat{y}$ components of $\overline{\rho}$ are independent, and that the plant locations are independent of each other, this phase term is evaluated as

$$\begin{aligned}&\langle\exp[i2k_0\overline{k}_\rho\cdot(\overline{\rho}_n-\overline{\rho}_m)]\rangle_{n\neq m} \\ &\quad= \left|\frac{i\left(e^{i2k^i_y y_{\max}} - e^{i2k^i_y y_{\min}}\right)}{k^i_y(y_{\min}-y_{\max})}\right|^2 \left|\sqrt{2}e^{-2(k^i_x\sigma_x)^2}\right|^2.\end{aligned} \tag{18}$$

This function, and thus the total scattering expressed by (17), is highly dependent on incidence angle and the statistics of the

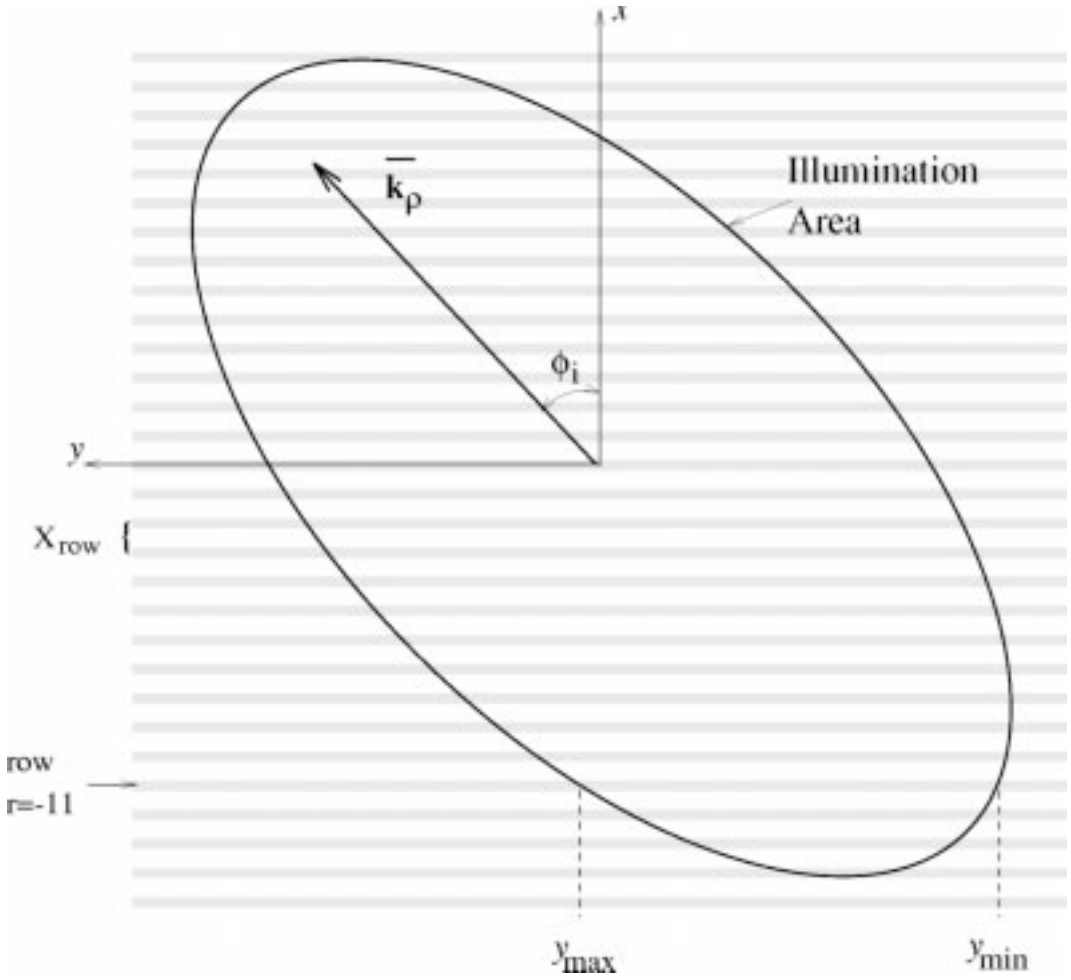

Fig. 11. Simple illumination pattern over a field of grass plants planted in rows at periodic intervals of distance X_{row}. This illumination area is defined by the illumination pattern and/or the ambiguity function of the radar.

row section. If $k_0\sigma_x$ and $k_y^i(y_{\min} - y_{\max})$ are small (occurring when $\sigma_x \ll \lambda$ and ϕ_i is small), then the above expression and thus the coherent scattering term can be significant.

The scattering from an area A encompassing a section of row-structured plants can therefore be modeled as the scattering from a collection of row sections located at $\overline{\rho}_{row}^r = rX_{row}\hat{x}$, where X_{row} is the spacing between adjacent rows and r is an integer value (Fig. 11)

$$\langle S_{\chi\psi}^{canopy} S_{\lambda\mu}^{*canopy}\rangle = \sum_{r=-N_{row}/2}^{N_{row}/2} \langle S_{\chi\psi}^{row} S_{\lambda\mu}^{*row}\rangle_r + \sum_{r=-N_{row}/2}^{N_{row}/2} \sum_{s=-N_{row}/2, r\neq s}^{N_{row}/2} \cdot \langle S_{\chi\psi}^{row}\rangle_r \langle S_{\lambda\mu}^{*row}\rangle_s e^{i2k_x^i X_{row}(r-s)} \quad (19)$$

where $\langle S_{\chi\psi}^{row}\rangle_r$ is the average scattered field of the row

$$\langle S_{\chi\psi}^{row}\rangle_r = N_{plants}^r \langle S_{\chi\psi}^{plant}\rangle \langle \exp[i2k_0\overline{k}_\rho \cdot \overline{\rho}_{plant}]\rangle_r. \quad (20)$$

The phase term in (20) is not written as an expected value, as the rows are modeled as a periodic array with spacing X_{row}. Because of this periodicity, the rows generate a Bragg scattering phenomenon [18, pp. 515–525], with the average scattered field from each row constructively adding in phase at a set of specific incidence angles. Note only a finite number of nonzero modes can occur between $\theta_i = \pi/2$ and $\theta_i = \pi$, and if $k_0 X_{row} < \pi$ then no nonzero modes occur. From (19), it is apparent that the effect of this Bragg scattering on the total scattering depends on the relative magnitude of $\langle S_{\chi\psi}^{row}\rangle$. If the average scattered field of a single row is small, then no Bragg effects will be observable.

Likewise, periodicity of the soil will result in Bragg scattering modes from the underlying surface, resulting in a more complex coherent wave than described by the spicular response of Fig. 3. For periodic soils, the complex reflection coefficient R, describing the spicular reflection at the soil, would correspond to the zeroth-order Bragg scattering mode. The higher order Bragg scattering terms are therefore not included in the formulation, which could result in significant error if the magnitude of the periodicity is not electrically small.

VI. Conclusions

A formulation describing the microwave scattering from a grassland canopy has been presented; it is an improvement over

earlier grass scattering models in two ways. The first improvement is the improved electromagnetic accuracy of the formulation. The model accounts for the coherent scattering effects that can result from a single plant, including the correlation in the scattered fields from dissimilar scattering mechanisms and dissimilar plant elements. The model also accounts for the nonuniform illumination of the long plant elements and determines the scattering for the overall canopy structure, including the coherent effects of cultural grasses planted in periodic rows. Although the incoherent scattering terms are likely dominant when compared to any *individual* coherent scattering term, the collection of coherent terms, due to their great numbers, may in certain circumstances be a significant portion of the overall scattered power.

The other improvement provided by this model is the ability to consider the physical structure of grassland elements and canopies accurately. Both the curvature and the cross section of the long, thin elements that constitute a grass canopy can be accurately reflected in the model, and the spatial distribution of these elements can likewise be accurately modeled (as opposed to assuming a uniform distribution). A key to these improvements is the ability to model the thin constituents elements as line dipoles, as the polarizability of these dipoles has been evaluated for blade-shaped cross sections.

APPENDIX

The propagation as given in (4) and (5) is defined in terms of $k_1 z$ or $k_1(z+2d)$. However, the propagation value k_1 is likely a function of vertical dimension z in a real grassland canopy, where the shape, size, and structure of the constituent plants change as a function of height. As a result, the propagation term $k_1 z$, for example, is more generally described as

$$\int_0^z k_1(z')\,dz'. \tag{21}$$

Since grassland vegetation is a sparse scattering medium, Foldy's approximation [19, pp. 458–461] is applicable. Likewise, grass plants are assumed azimuthally symmetric about the z axis. Therefore using the orthogonal polarization vectors $\hat{h}$ and $\hat{v}$ ($\hat{h}\cdot\hat{z}=\hat{h}\cdot\hat{v}=0$), the complex propagation constant within the vegetation for polarization $\psi \in \{h, v\}$ can be described as $k_1(z) = k_0 - \imath M_\psi(z)$, where M_ψ is related to the average forward scattering of the constituent elements ($\langle S_{\chi\psi}(k_0^s = k_0^i)\rangle$). For the long, thin elements found in grassland vegetation, we again use the concept of a differential line dipole to find

$$\begin{aligned} M_{\psi\psi}(\hat{k_0^i}) &= \frac{\imath 2\pi n_o}{k_0}\langle S_{\chi\psi}(k_0^s = k_0^i)\rangle \\ &= M_{\psi\psi}(z) \\ &= \frac{\imath N_{epa}(z) k_0^3}{2}\langle \hat{\psi}\cdot\mathcal{P}^{2d}(z)\cdot\hat{\psi}(d\ell/dz)\rangle \end{aligned} \tag{22}$$

where N_{epa} is the average number of elements intersecting a unit area of the vegetation layer a height z, and ℓ is the distance along the thin element axis. Therefore, $\int_0^z k_1(z')\,dz' = k_0 - \imath\tau_\chi(z)$, where $\tau_\chi(z)$ is

$$\tau_\chi(z) = \int_0^z M_{\psi\psi}(z)\,dz'. \tag{23}$$

Inserting this formulation into (4) and (5), the propagation paths associated with each of the four scattering mechanisms (Fig. 2) can be expressed in terms of the arbitrary polarization pair $\chi\psi = \{vv, hv, vh, hh\}$

$$\begin{aligned} \Phi^1_{\chi\psi} = \exp\Bigg[&\imath 2\left(k_x^i x^\ell + k_y^i y^\ell + k_z^i z^\ell\right) \\ &+ \frac{\tau_\chi(z^\ell)+\tau_\psi(z^\ell)}{\cos\theta}\Bigg] \end{aligned} \tag{24}$$

$$\begin{aligned} \Phi^2_{\chi\psi} = r_\psi \exp\Bigg[&\imath 2\left(k_x^i x^\ell + k_y^i y^\ell\right) \\ &+ \frac{\tau_\chi(z^\ell)-\tau_\psi(z^\ell)}{\cos\theta} - \imath 2k_z^i d + \frac{2\tau_\psi(-d)}{\cos\theta}\Bigg] \end{aligned} \tag{25}$$

$$\begin{aligned} \Phi^3_{\chi\psi} = r_\chi \exp\Bigg[&\imath 2\left(k_x^i x^\ell + k_y^i y^\ell\right) \\ &+ \frac{\tau_\psi(z^\ell)-\tau_\chi(z^\ell)}{\cos\theta} - \imath 2k_z^i d + \frac{2\tau_\psi(-d)}{\cos\theta}\Bigg] \end{aligned} \tag{26}$$

$$\begin{aligned} \Phi^4_{\chi\psi} = r_\chi r_\psi \exp\Bigg[&\imath 2\left(k_x^i x^\ell + k_y^i y^\ell - k_z^i z^\ell\right) \\ &- \frac{\tau_\chi(z^\ell)+\tau_\psi(z^\ell)}{\cos\theta} - \imath 2k_z^i d + \frac{2\tau_\psi(-d)}{\cos\theta}\Bigg] \end{aligned} \tag{27}$$

where r_χ, r_ψ are the complex Fresnel reflection coefficients associated with the proper polarization state.

REFERENCES

[1] S. H. Yueh, J. A. Kong, J. K. Jao, R. T. Shin, and T. Le Toan, "Branching model for vegetation," *IEEE Trans. Geosci. Remote Sensing*, vol. 30, pp. 390–401, Mar. 1992.

[2] G. Zhang, L. Tsang, and Z. Chen, "Collective scattering effects of trees generated by stochastic Lindenmayer systems," *Microw. Opt. Technol. Lett.*, vol. 11, no. 2, pp. 107–111, Feb. 1996.

[3] T. Le Toan, R. Robbes, L. Wang, N. Floury, K. Ding, J. A. Kong, and M. Fujita, "Rice crop mapping and monitoring using ERS-1 data based on experiment and modeling results," *IEEE Trans. Geosci. Remote Sensing*, vol. 35, pp. 41–56, Jan. 1994.

[4] Y. Lin and K. Sarabandi, "Coherent scattering model for forest canopies based on Monte Carlo simulation of fractal generated trees," in *Proc. Int. Geosci. Remote Sensing Symp.*, Lincoln, NE, May 27–31, 1996, pp. 1334–1336.

[5] L. Tsang, K. H. Ding, G. Zhang, C. C. Hsu, and J. A. Kong, "Backscattering enhancement and clustering effects of randomly distributed dielectric cylinders overlying a dielectric half-space based on Monte-Carlo simulations," *IEEE Trans. Antennas Propagat.*, vol. 43, pp. 488–499, May 1995.

[6] C. C. Hsu, H. C. Han, R. T. Shin, J. A. Kong, A. Beaudoin, and T. le Toan, "Radiative transfer theory for polarimetric remote sensing at P band," *Int. J. Remote Sens.*, vol. 12, no. 14, pp. 2943–2954, Sept. 1994.

[7] A. Toure, K. P. Thompson, G. Edwards, R. J. Brown, and B. G. Brisco, "Adaptation of the MIMICS backscattering model to the agricultural context—Wheat and canola at L and C bands," *IEEE Trans. Geosci. Remote Sensing*, vol. 32, pp. 47–61, Jan. 1994.

[8] J. van Zyl, "On the importance of polarization in radar scattering problems," Ph.D. dissertation, Calif. Inst. Technol., Pasadena, CA, Dec. 1985.

[9] S. Bakhtiari and R. Zoughi, "A model for backscattering characteristics of tall prairie grass canopies at microwave frequencies," *Remote Sens. Environ.*, vol. 36, pp. 137–147, 1991.
[10] S. S. Saatchi, D. M. Le Vine, and R. H. Lang, "Microwave backscattering and emission model for grass canopies," *IEEE Trans. Geosci. Remote Sensing*, vol. 32, pp. 177–186, Jan. 1994.
[11] K. Sarabandi and T. B. A. Senior, "Low-frequency scattering from cylindrical structures at oblique incidence," *IEEE Trans. Geosci. Remote Sensing*, vol. 28, pp. 879–885, Sept. 1990.
[12] J. M. Stiles and K. Sarabandi, "A scattering model for long, thin dielectric cylinders of arbitrary cross-section and electrical length," *IEEE Trans. Antennas Propagat.*, vol. 44, pp. 260–266, Feb. 1996.
[13] M. Whitt, "Microwave scattering from periodic row-structured vegetation," Ph.D. dissertation, Univ. Michigan, Ann Arbor, Nov. 1991.
[14] J. van Zyl and F. T. Ulaby, "Scattering matrix representation for simple targets," in *Radar Polarimetry for Geoscience Applications*, F. T. Ulaby and C. Elachi, Eds. Norwood, MA: Artech House, 1990.
[15] J. M. Stiles, K. Sarabandi, and F. T. Ulaby, "Microwave scattering model for grass blade structures," *IEEE Trans. Geosci. Remote Sensing*, vol. 31, no. 5, pp. 1051–1059, Sept. 1993.
[16] M. Whitt and F. T. Ulaby, "Radar response of periodic vegetation canopies," *Technol. Forecast. Social Change*, vol. 46, no. 3, pp. 1813–1848, July 1994.
[17] A. Tavakoli, K. Sarabandi, and F. T. Ulaby, "Horizontal propagation through periodic vegetation canopies," *IEEE Trans. Antennas Propagat.*, vol. 39, pp. 1014–1023, July 1991.
[18] J. A. Kong, *Electromagnetic Wave Theory*. New York: Wiley, 1990.
[19] L. Tsang, J. A. Kong, and R. T. Shin, *Theory of Microwave Remote Sensing*. New York: Wiley, 1985.

James M. Stiles (S'91–M'95–SM'97) was born in Kansas City, MO, on June 4, 1961. He received the B.S. degree in electrical engineering from the University of Missouri, Columbia, in 1983, the M.S. degree in electrical engineering from Southern Methodist University, Dallas, TX, in 1987, and the Ph.D. degree in electrical engineering from the University of Michigan, Ann Arbor, in 1996.

From 1983 to 1990, he was a Microwave Systems Design Engineer with Texas Instruments, Dallas, and from 1990 to 1996, he was a Graduate Research Assistant in the Radiation Laboratory, University of Michigan. Since 1996, he has been an Assistant Professor at the University of Kansas, where he is a Member of the Radar Systems and Remote Sening Laboratory. His research interests include radar remote sensing of vegetation, propagation and scattering in random media, ground penetrating radar, and radar signal processing.

Kamal Sarabandi (S'87–M'90–SM'93–F'00) received the B.S. degree in electrical engineering from Sharif University of Technology, Tehran, Iran, in 1980 and the M.S.E. degree in electrical engineering, the M.S. degree in mathematics, and the Ph.D. degree in electrical engineering, in 1984, 1989, and 1989, respectively, from the University of Michigan, Ann Arbor.

From 1980 to 1984, he worked as a Microwave Engineer in the Telecommunication Research Center, Iran. He is presently an Associate Professor in the Department of Electrical Engineering and Computer Science, University of Michigan. He has 18 years of experience with microwave sensors and radar systems. In the past eight years, he has served as the Principal Investigator and Co-Investigator on many projects sponsored by NASA, JPL, ARO, ONR, ARL, and GM all related in one way or the other to microwave and millimeter wave radar remote sensing. He has published many book chapters and more than 80 papers in refereed journals on electromagnetic scattering, random media modeling, microwave measurement techniques, radar calibration, application of neural networks in inverse scattering problems, and microwave sensors. He has also had more than 140 papers and invited presentations in national and international conferences and symposia on similar subjects.

Dr. Sarabandi is listed in *American Men & Women of Science* and *Who's Who in Electromagnetics*. He has been a member of the IEEE GEOSCIENCE AND REMOTE SENSING AdCom since January 1998 and has served as the Chairman of the Geoscience and Remote Sensing Society, Southeastern Michigan chapter, from 1992 to 1998. He is also a member of Commission F of URSI and of The Electromagnetic Academy. He was a recipient of the 1996 Teaching Excellence Award, the 1997 Henry Russel Award from the Regent of The University of Michigan, and the 1999 GAAC Distinguished Lecturer Award from the German Federal Ministry for Education, Science, and Technology.